

Supporting Information

**Synthesis of a Series of Coordination Polymers Based on
Mixed Ligands to Tune the Structural Dimension**

Xinyu Cao, Bao Mu, Rudan Huang*

Key Laboratory of Cluster Science of Ministry of Education, School of Chemistry, Beijing Institute of Technology, Beijing 100081, PR China E-mail: huangrudan1@bit.edu.cn

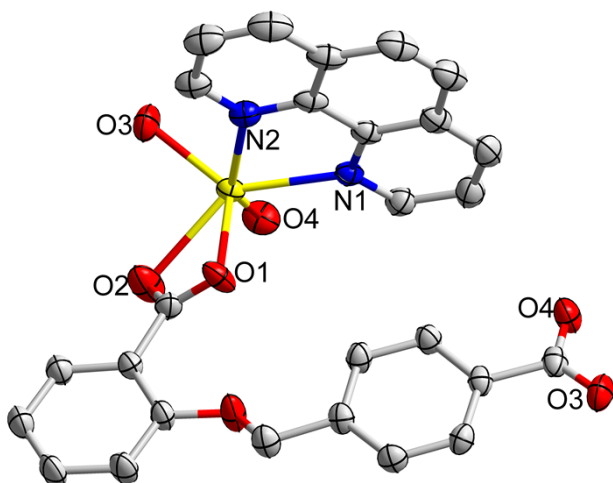


Figure S1. The coordination environment of Mn(II) in complex **1** with the ellipsoids drawn at the 30% probability level. Hydrogen atoms are omitted for clarity.

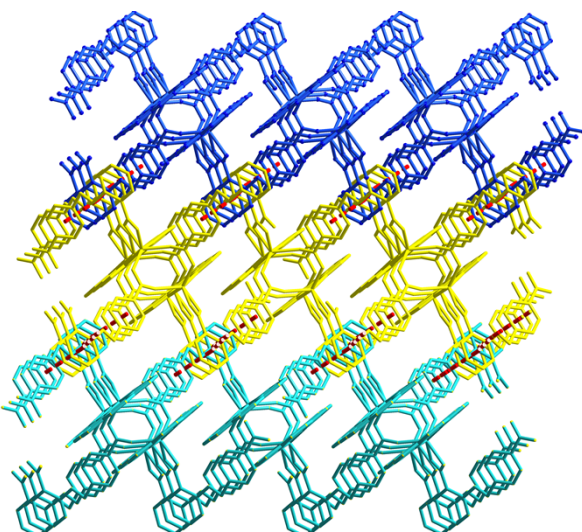


Figure S2. 3D supramolecular structure of **1** constructed by $\pi \cdots \pi$ stacking interactions (red lines: $\pi \cdots \pi$ stacking interactions; turquoise, yellow and light blue represent three 2D layers, respectively).

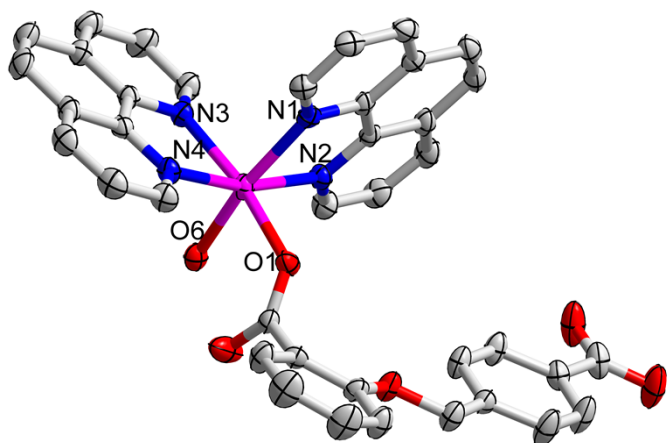


Figure S3. The coordination environment of Co(II) in complex **2** with the ellipsoids drawn at the 30% probability level. Hydrogen atoms and water molecules are omitted for clarity.

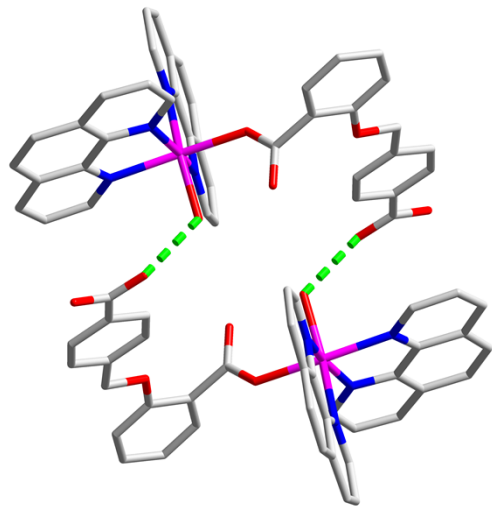


Figure S4. The supramolecular dimer cage of **2** constructed by hydrogen bonding. (bright green lines)

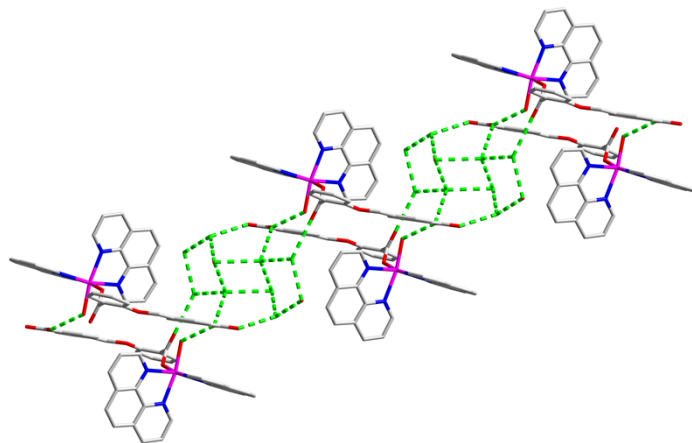


Figure S5. 1D supramolecular chain of **2** constructed by hydrogen bonding (bright lines).

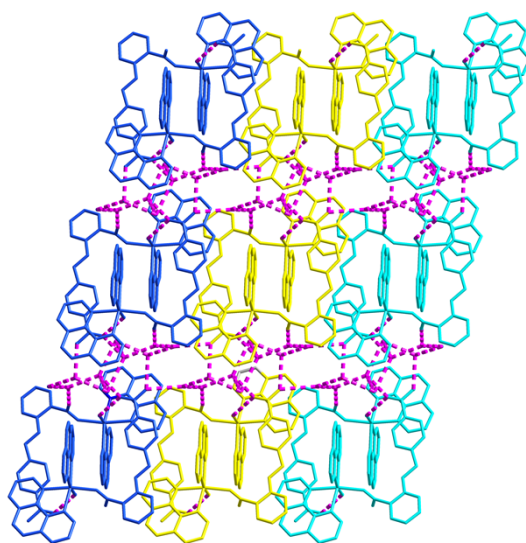


Figure S6. 2D supramolecular layer of **2** formed through hydrogen bonding along *b* axis. (pink lines: hydrogen bond; turquoise, yellow and light blue represent three 1D supramolecular chains, respectively)

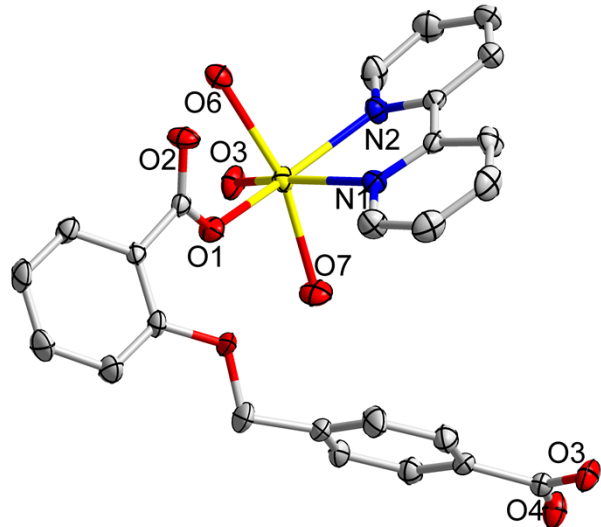


Figure S7. The coordination environment of Mn(II) in complex **5** with the ellipsoids drawn at the 30% probability level. Hydrogen atoms are omitted for clarity.

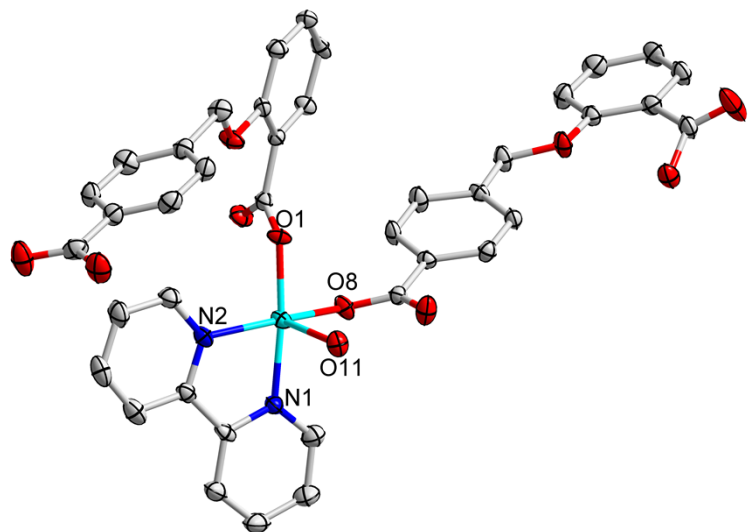


Figure S8. The coordination environment of Co(II) in complex **7** with the ellipsoids drawn at the 30% probability level. Hydrogen atoms and water molecules are omitted for clarity.

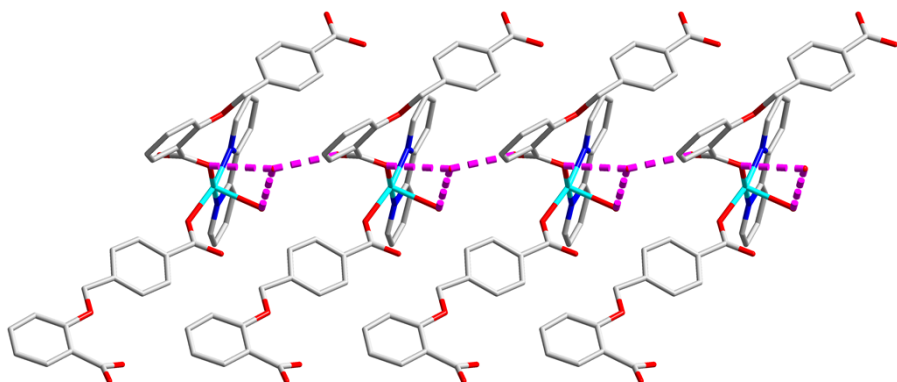


Figure S9. 1D supramolecular chain of **7** constructed by hydrogen bonding (pink lines) along *c* axis.

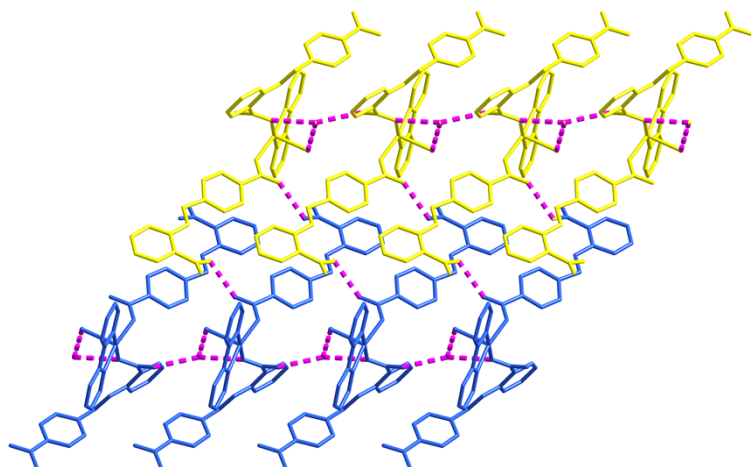


Figure S10. 2D supramolecular layer of **7** constructed by hydrogen bonding along *c* axis. (pink lines: hydrogen bond; yellow and light blue represent two 1D supramolecular chains, respectively).

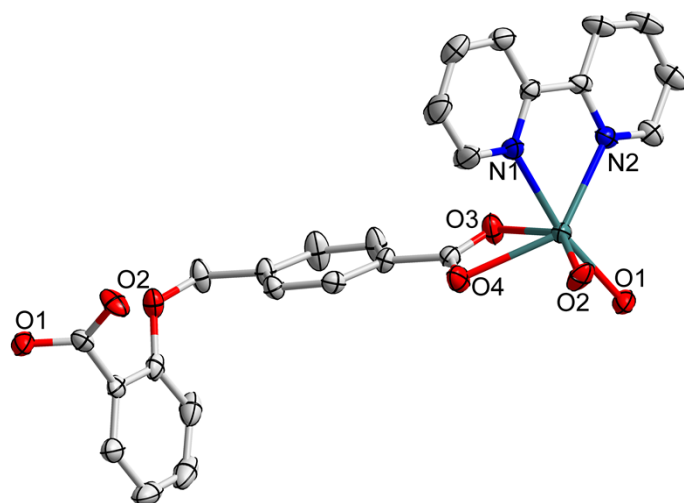


Figure S11. The coordination environment of Cd(II) in complex **8** with the ellipsoids drawn at the 30% probability level. Hydrogen atoms are omitted for clarity.

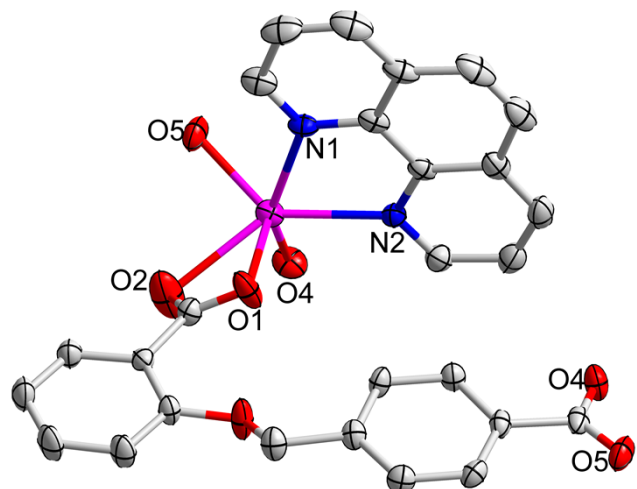


Figure S12. The coordination environment of Mn(II) in complex **3** with the ellipsoids drawn at the 30% probability level. Hydrogen atoms are omitted for clarity.

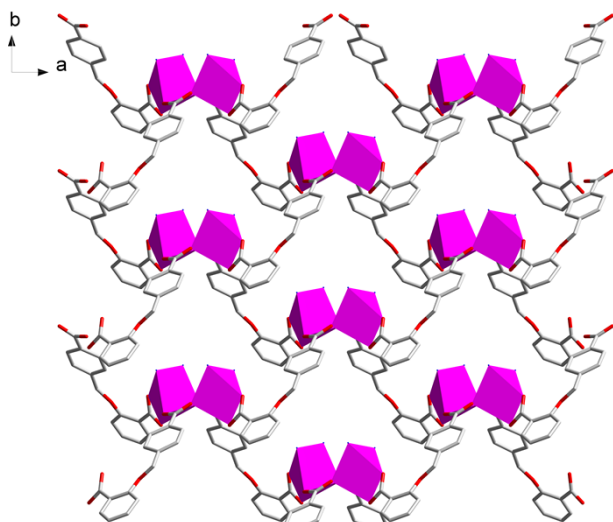


Figure S13. The 2D wave-like layer of **3**, viewed along the *c* axis (phen ligands are omitted for clarity).

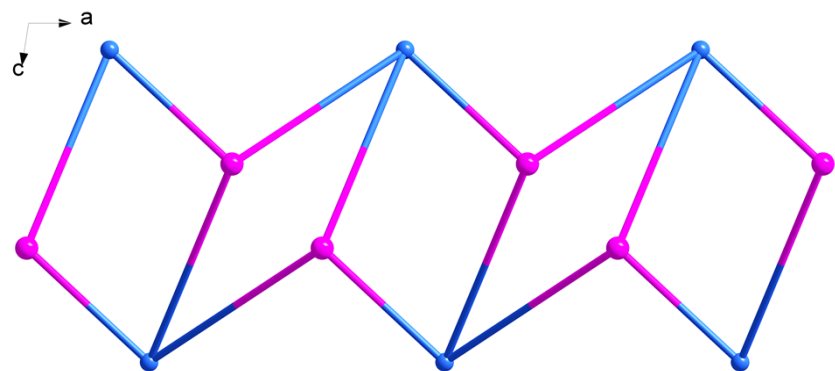


Figure S14. Schematic illustrating the 2D network of complex **3**. Color code: yellow, Mn, cob²⁺ ligand: red.

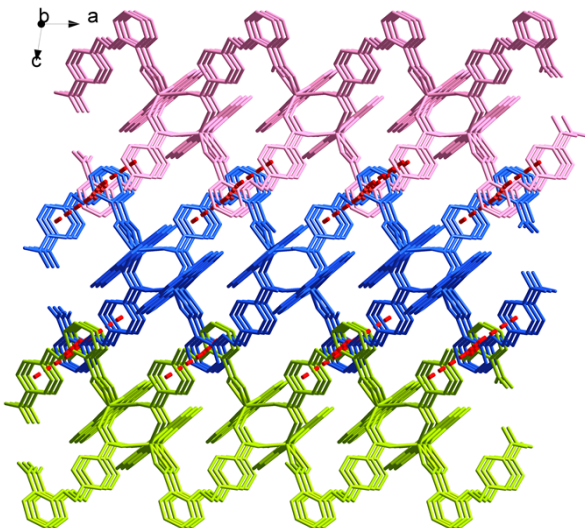


Figure S15. 3D supramolecular structure of **3** constructed by $\pi\cdots\pi$ stacking interactions (red lines: $\pi\cdots\pi$ stacking interactions; turquoise, yellow and light blue represent three 2D layers, respectively).

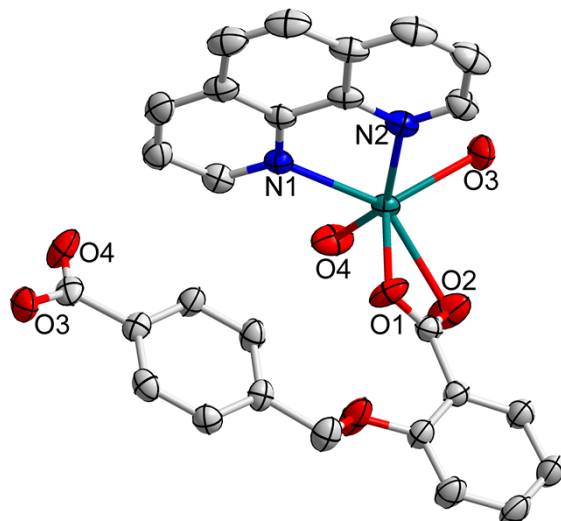


Figure S16. The coordination environment of Mn(II) in complex **4** with the ellipsoids drawn at the 30% probability level. Hydrogen atoms are omitted for clarity.

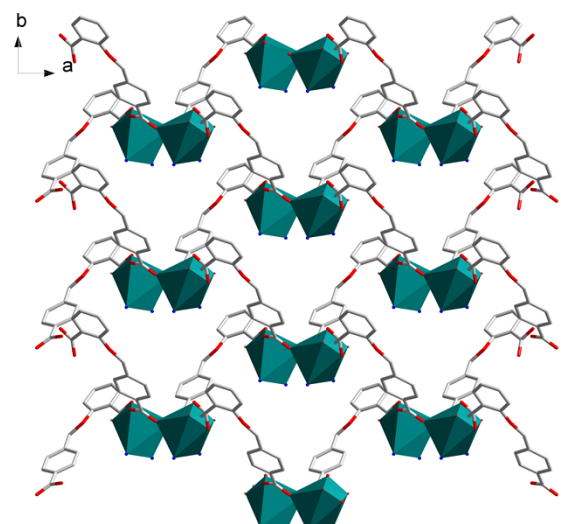


Figure S17. The 2D wave-like layer of **4**, viewed along the *c* axis (phen ligands are omitted for clarity).

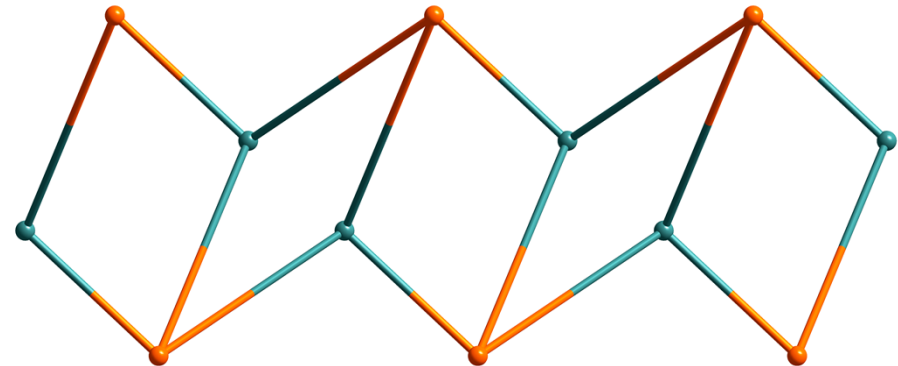


Figure S18. Schematic illustrating the 2D network of complex **4**. Color code: yellow, Mn, cob²⁺-ligand: red.

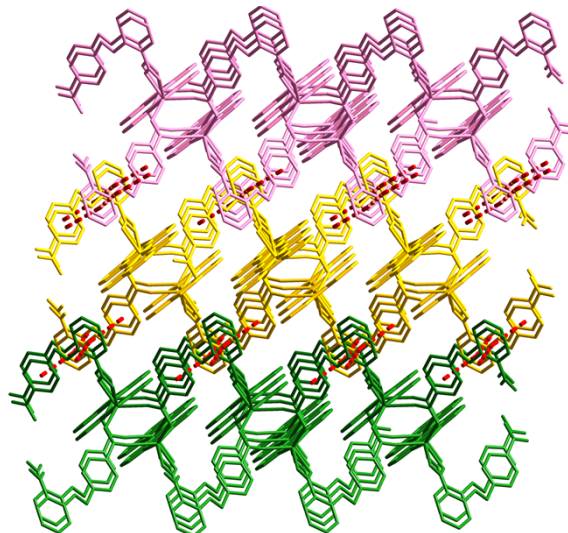


Figure S19. 3D supramolecular structure of **4** constructed by $\pi \cdots \pi$ stacking interactions (red lines: $\pi \cdots \pi$ stacking interactions; turquoise, yellow and light blue represent three 2D layers, respectively).

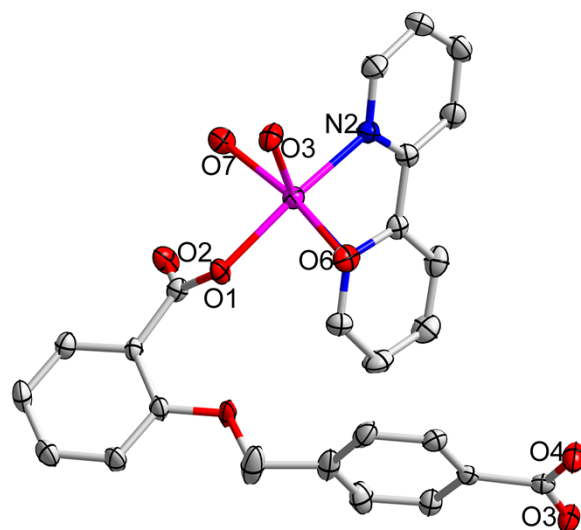


Figure S20. The coordination environment of Mn(II) in complex **6** with the ellipsoids drawn at the 30% probability level. Hydrogen atoms are omitted for clarity.

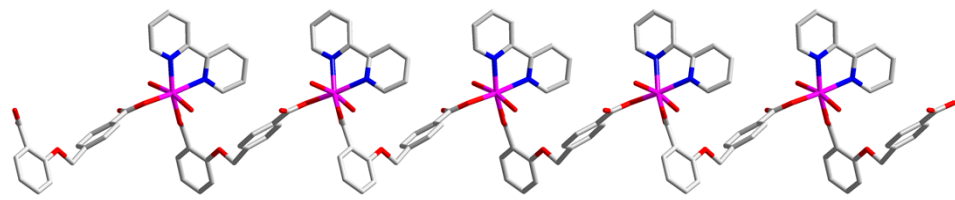


Figure S21. 1D zigzag chain of complex **6**, viewed along the *b* axis, hydrogen atoms are omitted for clarity.

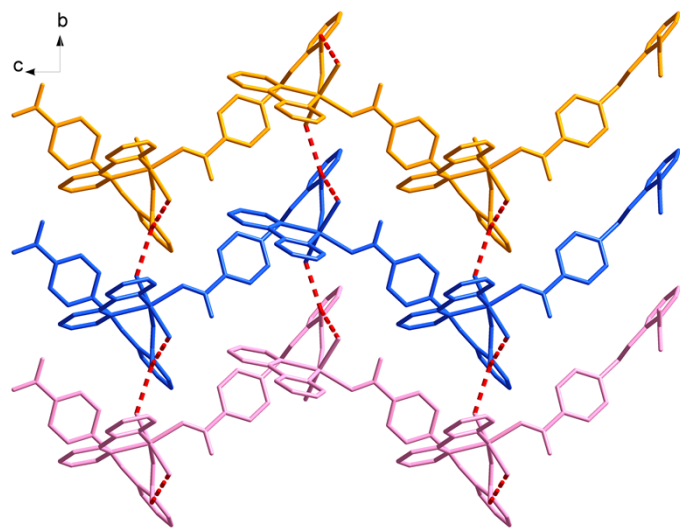


Figure S22. 2D supramolecular layer of **6** formed by hydrogen bonding along *b* axis. (pink lines: hydrogen bond; turquoise, yellow and light blue represent three 1D supramolecular chains, respectively)

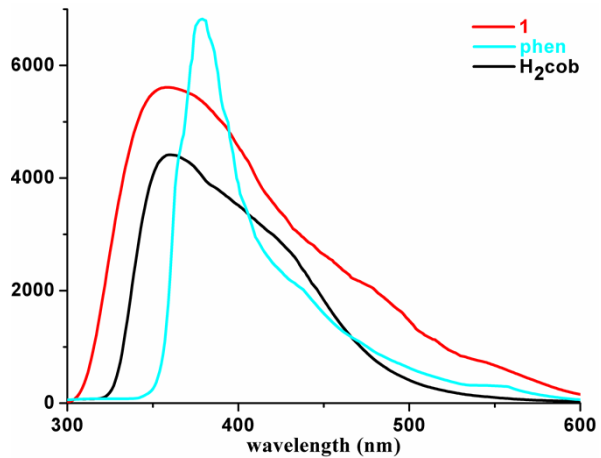


Figure S23. Solid state emission spectra of complex **1**, H₂cob and phen at room temperature.

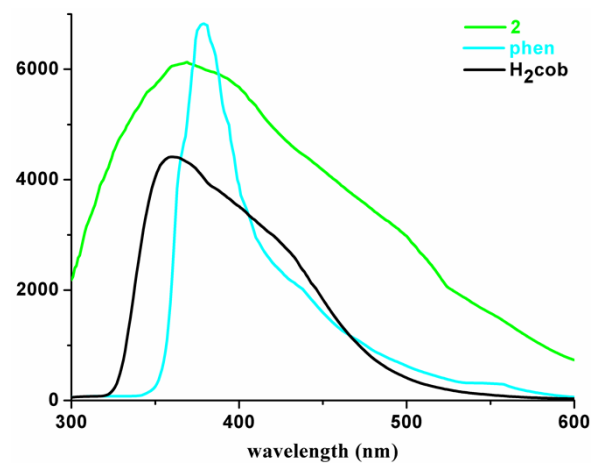


Figure S24. Solid state emission spectra of complex **2**, H₂cob and phen at room temperature.

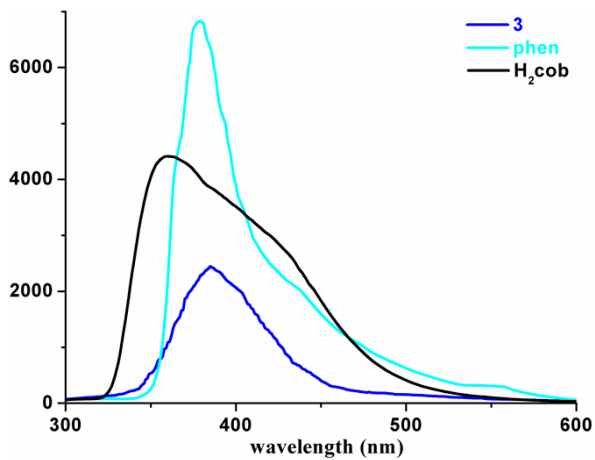


Figure S25. Solid state emission spectra of complex **3**, H₂cob and phen at room temperature.

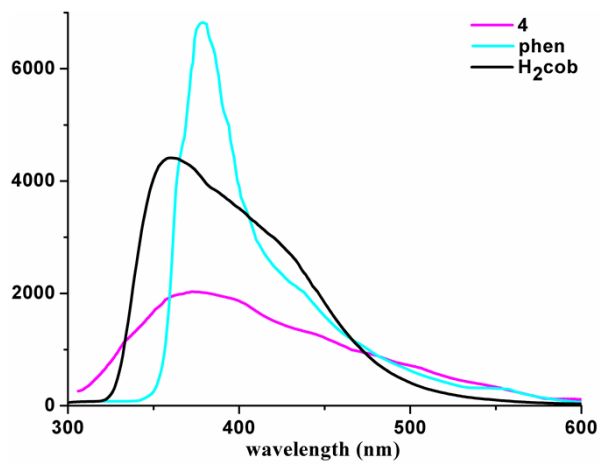


Figure S26. Solid state emission spectra of complex 4, H₂cob and phen at room temperature.

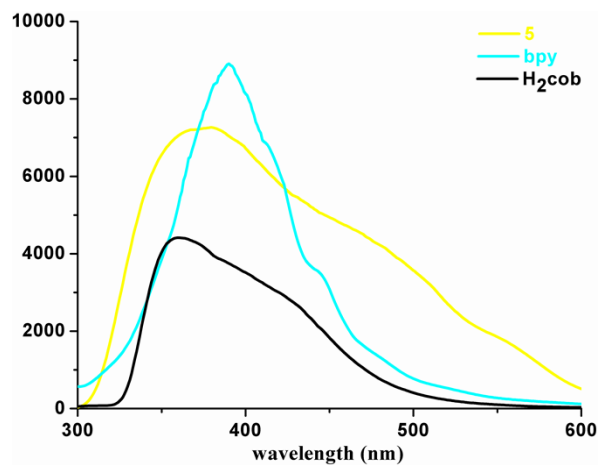


Figure S27. Solid state emission spectra of complex 5, H₂cob and bpy at room temperature.

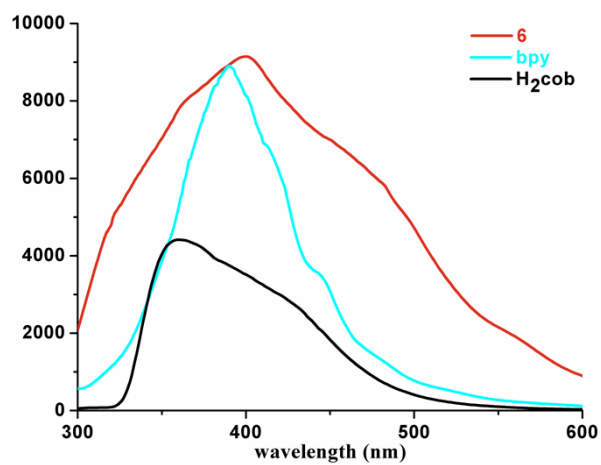


Figure S28. Solid state emission spectra of complex 6, H₂cob and bpy at room temperature.

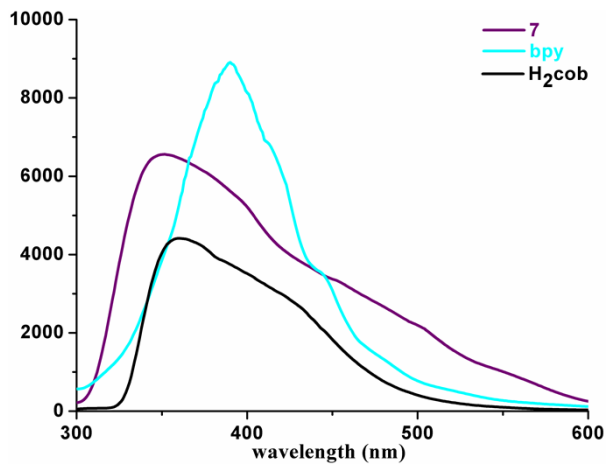


Figure S29. Solid state emission spectra of complex 7, H₂cob and bpy at room temperature.

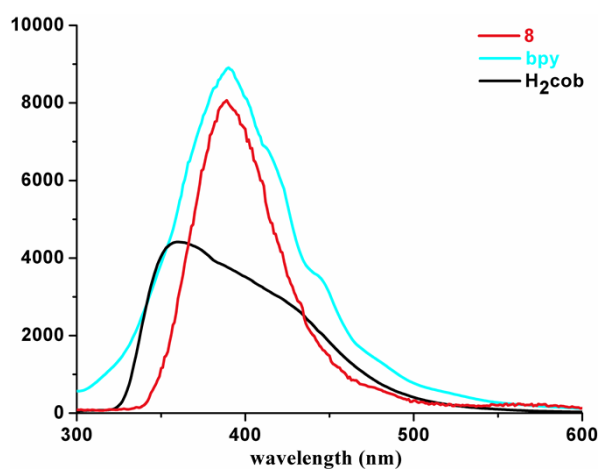


Figure S30. Solid state emission spectra of complex 8, H₂cob and bpy at room temperature.

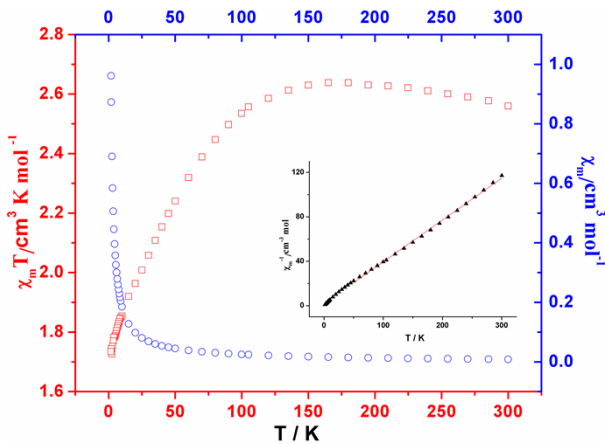


Figure S31. Temperature dependence of magnetic susceptibilities in the form of the χ_m and $\chi_m T$ versus T for **2** at 1000 Oe. Inset: χ_m^{-1} versus T; the solid line is fit to the experimental data.

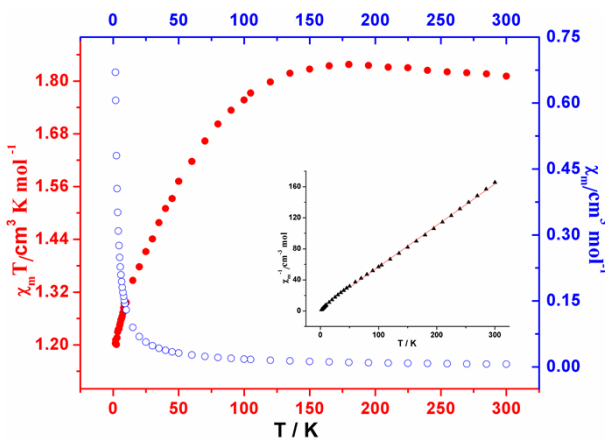


Figure S32. Temperature dependence of magnetic susceptibilities in the form of the χ_m and $\chi_m T$ versus T for **3** at 1000 Oe. Inset: χ_m^{-1} versus T; the solid line is fit to the experimental data.

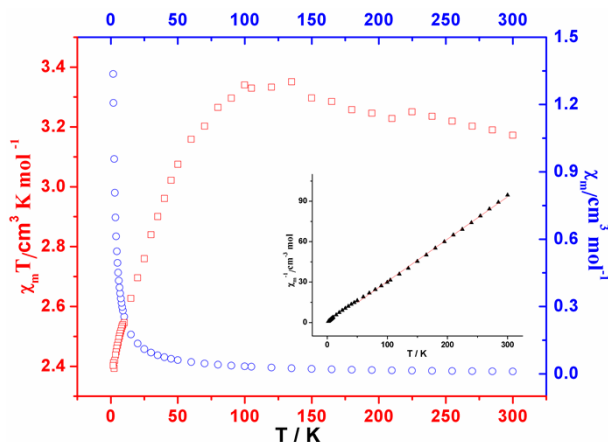


Figure S33. Temperature dependence of magnetic susceptibilities in the form of the χ_m and $\chi_m T$ versus T for **6** at 1000 Oe. Inset: χ_m^{-1} versus T; the solid line is fit to the experimental data.

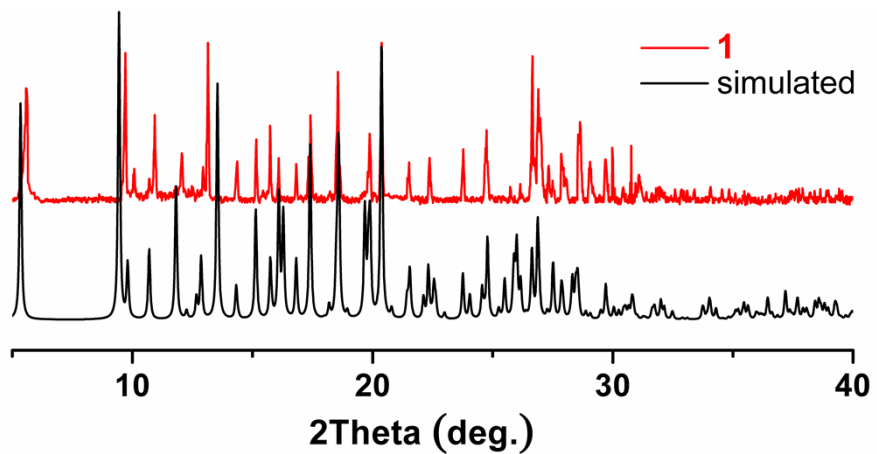


Figure S34. XRPD experimental and calculated patterns for complex 1.

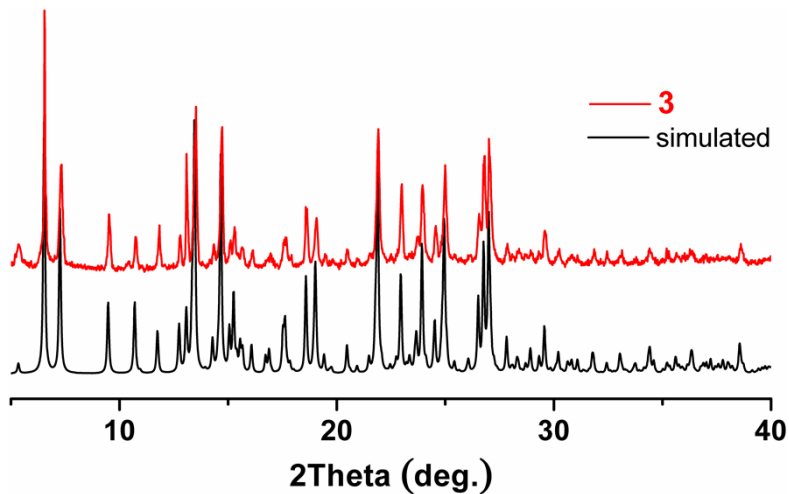


Figure S35. XRPD experimental and calculated patterns for complex 3.

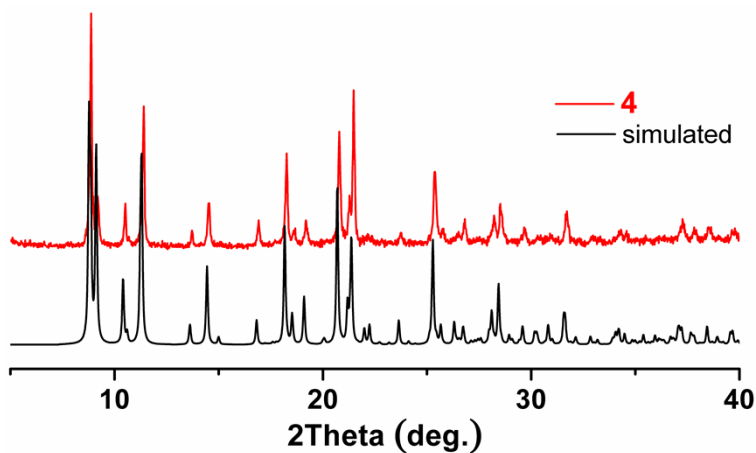


Figure S36. XRPD experimental and calculated patterns for complex 4.

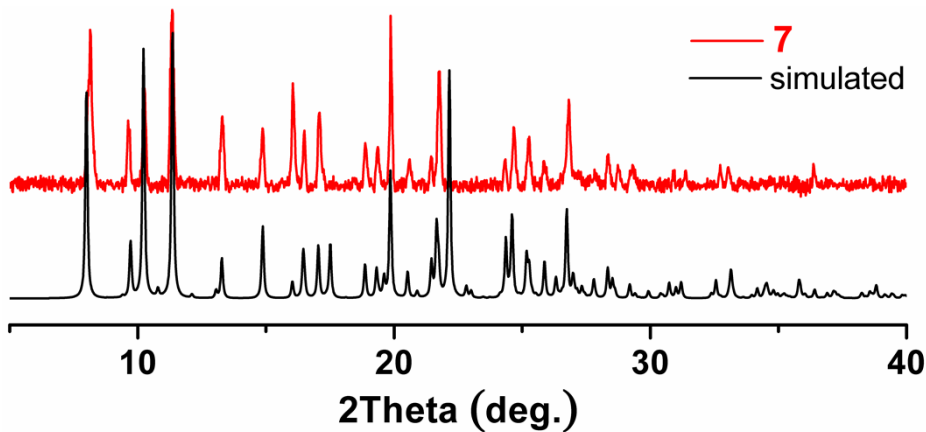


Figure S37. XRPD experimental and calculated patterns for complex **7**.

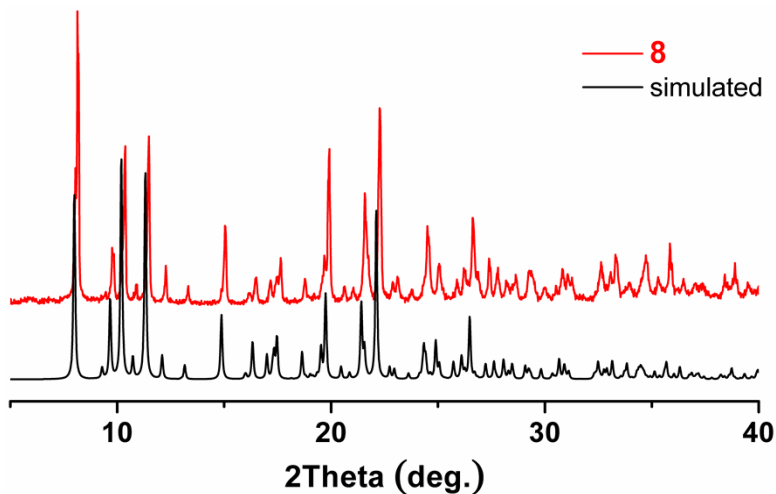


Figure S38. XRPD experimental and calculated patterns for complex **8**.

Gas sorption studies.

For gas adsorption studies, the sample of **2**, **5** and **6** were exchanged by CH_2Cl_2 after soaking these complexes in CH_2Cl_2 for 48 h, and the exchanged samples were further activated by heating at 120 °C for 12 h under vacuum conditions, giving three activated complexes.

According to the N_2 adsorption data, the Brunauer–Emmett–Teller (BET) surface areas of **2**, **5** and **6** are 22.88, 18.59 and 6.38 m^2/g , respectively, and their total pore volumes are 0.35, 0.07 and 0.09 cm^3/g .

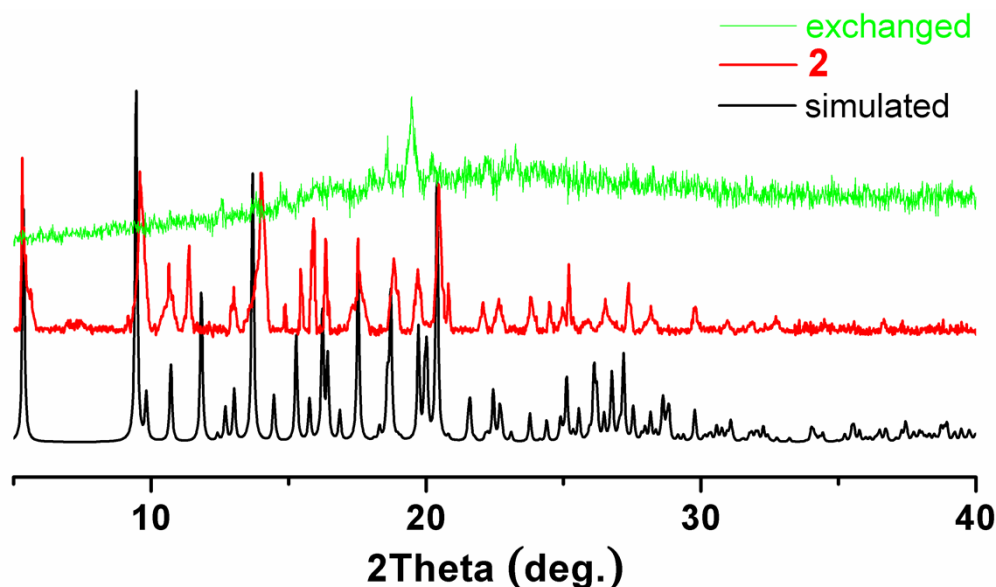


Figure S39. PXRD experimental, exchanged and calculated patterns for complex **2**.

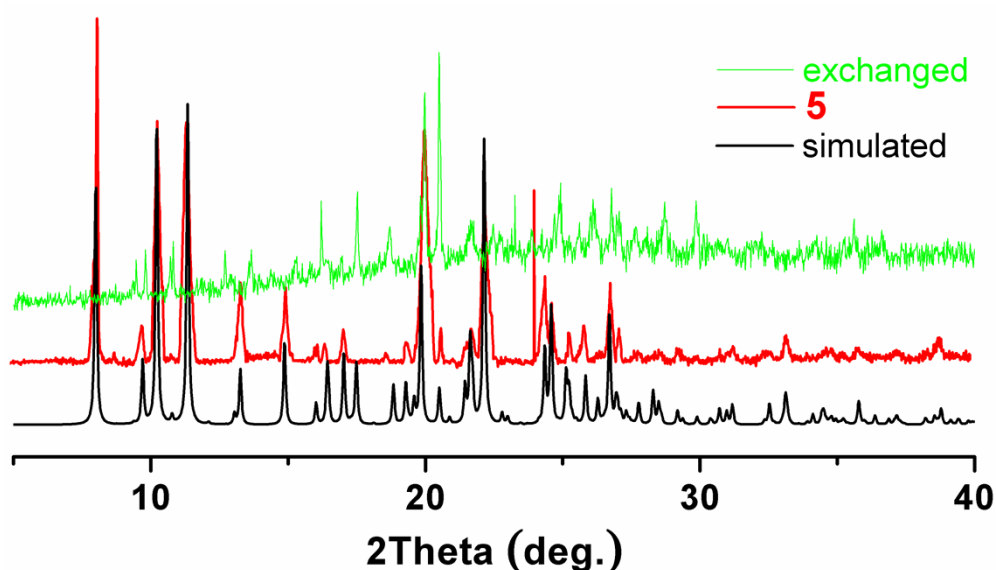


Figure S40. PXRD experimental, exchanged and calculated patterns for complex **5**.

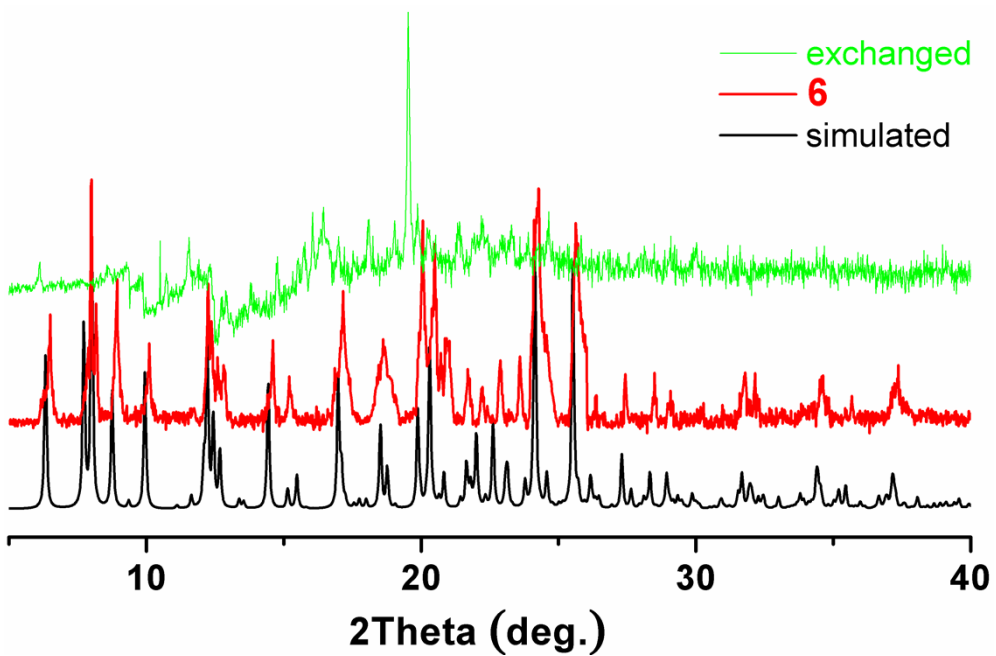


Figure S41. PXRD experimental, exchanged and calculated patterns for complex **6**.

Table S1. Selected Bond Lengths (\AA) and Angles (deg) for **1–8**.

1			
Mn(1)-O(3)#1	2.086(3)	Mn(1)-O(4)#2	2.099(2)
Mn(1)-O(1)	2.141(4)	Mn(1)-N(2)	2.322(3)
Mn(1)-N(1)	2.335(3)	Mn(1)-O(2)	2.452(4)
O(3)#1-Mn(1)-O(4)#2	103.35(11)	O(3)#1-Mn(1)-O(1)	119.56(16)
O(4)#2-Mn(1)-O(1)	113.42(18)	O(3)#1-Mn(1)-N(2)	80.01(10)
O(4)#2-Mn(1)-N(2)	147.04(11)	O(1)-Mn(1)-N(2)	91.76(17)
O(3)#1-Mn(1)-N(1)	134.47(10)	O(4)#2-Mn(1)-N(1)	85.20(10)
O(1)-Mn(1)-N(1)	95.94(13)	N(2)-Mn(1)-N(1)	70.74(10)
O(3)#1-Mn(1)-O(2)	85.34(12)	O(4)#2-Mn(1)-O(2)	82.62(15)
O(1)-Mn(1)-O(2)	55.72(17)	N(2)-Mn(1)-O(2)	130.22(15)
N(1)-Mn(1)-O(2)	140.13(11)		

2			
Co(1)-O(6)	2.076(3)	Co(1)-O(1)	2.096(3)
Co(1)-N(4)	2.124(3)	Co(1)-N(2)	2.142(3)
Co(1)-N(3)	2.158(3)	Co(1)-N(1)	2.160(3)
O(6)-Co(1)-O(1)	88.03(11)	O(6)-Co(1)-N(4)	99.07(11)
O(1)-Co(1)-N(4)	93.88(12)	O(6)-Co(1)-N(2)	91.80(11)
O(1)-Co(1)-N(2)	95.95(11)	N(4)-Co(1)-N(2)	165.58(13)
O(6)-Co(1)-N(3)	87.91(11)	O(1)-Co(1)-N(3)	170.03(10)
N(4)-Co(1)-N(3)	77.79(12)	N(2)-Co(1)-N(3)	93.28(11)
O(6)-Co(1)-N(1)	168.93(11)	O(1)-Co(1)-N(1)	90.53(11)
N(4)-Co(1)-N(1)	91.97(12)	N(2)-Co(1)-N(1)	77.43(12)
N(3)-Co(1)-N(1)	95.16(12)		

3			
Co(1)-O(5)#1	2.087(4)	Co(1)-O(4)	2.102(4)
Co(1)-O(1)	2.139(4)	Co(1)-N(1)	2.323(4)
Co(1)-N(2)	2.329(4)		
O(5)#1-Co(1)-O(4)	103.54(17)	O(5)#1-Co(1)-O(1)	120.05(18)
O(4)-Co(1)-O(1)	112.31(18)	O(5)#1-Co(1)-N(1)	79.76(16)
O(4)-Co(1)-N(1)	147.03(16)	O(1)-Co(1)-N(1)	92.85(16)
O(5)#1-Co(1)-N(2)	134.30(16)	O(4)-Co(1)-N(2)	85.23(16)
O(1)-Co(1)-N(2)	96.00(15)	N(1)-Co(1)-N(2)	70.72(16)

4			
Cd(1)-O(4)#1	2.220(3)	2.267(5)	2.267(5)
Cd(1)-O(3)	2.271(4)	Cd(1)-N(2)	2.373(4)
Cd(1)-N(1)	2.405(3)	Cd(1)-O(2)	2.441(5)
O(4)#1-Cd(1)-O(1)	108.8(3)	O(4)#1-Cd(1)-O(3)	105.76(13)
O(1)-Cd(1)-O(3)	122.2(3)	O(4)#1-Cd(1)-N(2)	150.08(12)
O(1)-Cd(1)-N(2)	92.3(3)	O(3)-Cd(1)-N(2)	78.64(13)
O(4)#1-Cd(1)-N(1)	87.33(13)	O(1)-Cd(1)-N(1)	95.4(2)
O(3)-Cd(1)-N(1)	131.26(12)	N(2)-Cd(1)-N(1)	69.27(13)

O(4)#1-Cd(1)-O(2)	84.0(3)	O(1)-Cd(1)-O(2)	53.85(19)
O(3)-Cd(1)-O(2)	86.3(2)	N(2)-Cd(1)-O(2)	126.0(3)
N(1)-Cd(1)-O(2)	142.3(2)		

5

Mn(1)-O(3)#1	2.121(3)	Mn(1)-O(1)	2.148(3)
Mn(1)-O(7)	2.210(3)	Mn(1)-N(2)	2.266(4)
Mn(1)-O(6)	2.268(3)	Mn(1)-N(1)	2.281(3)
O(3)#1-Mn(1)-O(1)	108.08(12)	O(3)#1-Mn(1)-O(7)	86.23(11)
O(1)-Mn(1)-O(7)	82.82(12)	O(3)#1-Mn(1)-N(2)	92.91(12)
O(1)-Mn(1)-N(2)	158.01(11)	O(7)-Mn(1)-N(2)	105.62(13)
O(3)#1-Mn(1)-O(6)	86.62(12)	O(1)-Mn(1)-O(6)	85.83(11)
O(7)-Mn(1)-O(6)	164.00(12)	N(2)-Mn(1)-O(6)	89.03(12)
O(3)#1-Mn(1)-N(1)	158.47(11)	O(1)-Mn(1)-N(1)	89.83(12)
O(7)-Mn(1)-N(1)	84.23(11)	N(2)-Mn(1)-N(1)	71.28(13)
O(6)-Mn(1)-N(1)	107.03(12)		

6

Co(1)-O(3)#1	2.047(3)	Co(1)-O(1)	2.078(3)
Co(1)-N(2)	2.134(4)	Co(1)-N(1)	2.143(4)
Co(1)-O(6)	2.149(3)	Co(1)-O(7)	2.184(3)
O(3)#1-Co(1)-O(1)	101.46(12)	O(3)#1-Co(1)-N(2)	94.46(14)
O(1)-Co(1)-N(2)	162.70(14)	O(3)#1-Co(1)-N(1)	162.17(13)
O(1)-Co(1)-N(1)	90.78(13)	N(2)-Co(1)-N(1)	75.40(14)
O(3)#1-Co(1)-O(6)	85.11(13)	O(1)-Co(1)-O(6)	83.86(13)
N(2)-Co(1)-O(6)	104.41(14)	N(1)-Co(1)-O(6)	83.35(13)
O(3)#1-Co(1)-O(7)	88.87(14)	O(1)-Co(1)-O(7)	87.19(12)
N(2)-Co(1)-O(7)	86.37(13)	N(1)-Co(1)-O(7)	104.79(14)
O(6)-Co(1)-O(7)	168.00(13)		

7

Cu(1)-O(8)	1.932(3)	Cu(1)-O(1)	1.935(3)
Cu(1)-N(1)	1.998(4)	Cu(1)-N(2)	2.009(4)
Cu(1)-O(11)	2.284(3)		
O(8)-Cu(1)-O(1)	91.91(14)	O(8)-Cu(1)-N(1)	92.78(16)
O(1)-Cu(1)-N(1)	173.92(18)	O(8)-Cu(1)-N(2)	164.54(17)
O(1)-Cu(1)-N(2)	93.85(16)	N(1)-Cu(1)-N(2)	80.65(18)
O(8)-Cu(1)-O(11)	97.78(14)	O(1)-Cu(1)-O(11)	93.54(13)
N(1)-Cu(1)-O(11)	89.66(15)	N(2)-Cu(1)-O(11)	96.17(15)

8

Cd(1)-O(1)	2.233(3)	Cd(1)-O(2)#1	2.244(3)
Cd(1)-N(2)	2.343(3)	Cd(1)-N(1)	2.354(3)
Cd(1)-O(3)	2.360(3)	Cd(1)-O(4)	2.382(2)
O(1)-Cd(1)-O(2)#1	92.09(10)	O(1)-Cd(1)-N(2)	101.55(11)
O(2)#1-Cd(1)-N(2)	123.02(10)	O(1)-Cd(1)-N(1)	169.51(11)
O(2)#1-Cd(1)-N(1)	88.18(11)	N(2)-Cd(1)-N(1)	69.74(12)
O(1)-Cd(1)-O(3)	90.84(10)	O(2)#1-Cd(1)-O(3)	145.98(10)

N(2)-Cd(1)-O(3)	89.40(10)	N(1)-Cd(1)-O(3)	94.80(10)
O(1)-Cd(1)-O(4)	104.37(9)	O(2) ^{#1} -Cd(1)-O(4)	91.14(10)
N(2)-Cd(1)-O(4)	135.86(10)	N(1)-Cd(1)-O(4)	86.10(10)
O(3)-Cd(1)-O(4)	55.41(10)		

Symmetry transformations used to generate equivalent atoms: #1 $x-1/2, y-1/2, z$; #2 $-x+1/2, y-1/2, -z+1/2$; #3 $x+1/2, y+1/2, z$; #4 $-x+1/2, y+1/2, -z+1/2$ for **1**; #1 $-x+1, y, -z+1/2$; #2 $-x+1/2, y-1/2, -z+1/2$; #3 $-x+1/2, y+1/2, -z+1/2$ for **3**; #1 $-x+1, y, -z+1/2$; #2 $x-1/2, y+1/2, z$; #3 $x+1/2, y-1/2, z$ for **4**; #1 $x, -y, z+1/2$; #2 $x, -y, z-1/2$ for **5**; #1 $x, -y+1, z+1/2$; #2 $x, -y+1, z-1/2$ for **6**; #1 $-x+2, y, -z+3/2$; #2 $x+1, y, z$; #3 $x-1, y, z$ for **8**.

Table S2. Hydrogen bonding interactions in H₂cob and **1–8**.

D–H···A	d(D···A) (Å)	∠D–H···A(°)
2		
O(6)–H(6B)···O(3)	2.6289	158
O(7)–H(7C)···O(2)	2.8762	159
O(7)–H(7D)···O(9)	2.7777	159
O(8)–H(8C)···O(7)	2.7614	172
O(8)–H(8D)···O(3)	2.7374	172
O(9)–H(9C)···O(4)	2.8309	160
O(9)–H(9D)···O(10)	2.8748	160
O(10)–H(10C)···O(4)	2.7226	178
O(10)–H(10D)···O(11)	2.7927	177
O(11)–H(11C)···O(8)	2.9948	157
O(11)–H(11D)···O(8)	2.9858	158
5		
O(7)–H(7A)···O(2)	2.6791	168
6		
O(6)–H(6A)···O(2)	2.6945	165
7		
O(4)–H(4)···O(3)	2.6133	168
O(6)–H(6)···O(9)	2.6134	139
O(11)–H(11B)···O(12)	2.7517	156
O(12)–H(12C)···O(1)	2.8413	154
O(12)–H(12C)···O(11)	2.7517	101